RSC Advances

ROYAL SOCIETY OF CHEMISTRY

www.rsc.org/advances

Journal Name

ARTICLE

Tunable properties of GO-doped CoFe₂O₄ nanofibers elaborated by Electrospinning

C. Eid,[a,†] E. Assaf,[a,b] R. Habchi,[a] P. Miele,[b] and M. Bechelany[b, †]

Cobalt ferrite ($CoFe_2O_4$) one-dimensional nanofibers doped with Graphene oxide (GO) were successfully synthesized for the first time via the electrospinning technique. The as-spun nanofibers were calcined at $600^{\circ}C$ for 3h with a slow heating rate of $2^{\circ}C/min^{-1}$. Their morphological and structural properties were studied by scanning electron microscopy (SEM), X-ray diffraction (XRD), Transmission Electron Microscopy, Energy-dispersive X-ray spectroscopy (EDX), and Raman spectroscopy. All GO-doped $CoFe_2O_4$ fibers showed pure spinel structure. The average fibers' diameter and the grain size were influenced by the GO weight amount. The effect of the Graphene oxide incorporation on the magnetic properties of the fibers was investigated by superconducting quantum interference device (SQUID) magnetometry. At room temperature, a slight enhancement of the saturation magnetization was detected while increasing the GO amount. Therefore, doping with GO is able to tune the magnetic properties of the $CoFe_2O_4$ fibers elaborated by the electrospinning technique.

Introduction

Nanoscale materials, particularly 1-D structures, are of a great technological interest mainly due to their anisotropic morphology and their high surface area to volume ratio [1-6]. Electrospinning is a simple and effective method to prepare 1D nanostructure including polymer nanofibers, inorganic nanofibers and composite nanofibers [7-9]. Many attempts have been successful to design and prepare ferrite nanofibers using this route [4, 10-11]. In fact, nanocrystalline ferrites with the general formula AFe_2O_4 (A = Mn, Co, Ni, Cu, or Zn) present interesting magnetic and electrical properties with chemical and thermal stabilities [12]. These materials are technologically important and have been used in many applications including magnetic recording media and magnetic fluids for the storage and/or retrieval of information, magnetic resonance imaging (MRI) enhancement, catalysis, magnetically guided drug delivery, sensors and pigments [13-14]. Cobalt ferrite ($CoFe_2O_4$) is one of the most important ferrites due to their large magnetocrystalline anisotropy, high coercivity, moderate saturation magnetization, chemical stability and mechanical hardness [12].

Recently, Graphene has attracted much attention because of its superior properties such as electrical, mechanical, thermal and chemical ones [15-18]. Graphene oxide (GO) is one of the most important Graphene derivatives. Unlike the Graphene, GO possesses a hydrophilic nature. As a result, GO readily forms stable colloidal suspensions of thin sheets which make the mixing process with the electrospun solution an easy task [19-20]. From the chemical point of view, the presence of oxygen functionalities at GO surface may be very interesting because they provide reactive sites for chemical modification. In fact, the polar oxygen functional groups of GO enhances the interfacial adhesion between GO and hydrophilic matrix [21-22].

The combination of magnetic nanostructure and Graphene becomes a hot topic of research in a wide variety of applications in catalysis, biomedical fields, and removal of contaminants from waste water [23]. Graphene-based hybrids containing magnetic NPs have been recently reported [24-25]. Also, Fe_3O_4-Graphene composite has been synthesized and used in dye removal from aqueous media [26]. Li *et al.* have successfully prepared magnetic $CoFe_2O_4$ functionalized Graphene nanocomposites by hydrothermal treatment of inorganic salts and thermal exfoliated Graphene sheets as an effective absorbent for removing methyl orange in water [27].

However, to our knowledge, there is no study concerning the preparation of a Graphene oxide-magnetic nanofiber nanocomposite. In this work, Electrospinning has been used as an effective way to generate $CoFe_2O_4$/GO nanofibers with tunable magnetic properties. The GO amount has been varied showing its direct effect on both magnetic properties and crystalline structure of the nanofibers.

a. *Research Platform for Nanosciences and Nanotechnologies, campus Pierre Gemayel, Fanar, Lebanese University, 90239, Lebanon.*
b. *Institut Européen des Membranes, UMR 5635 ENSCM UM CNRS, Université du Montpellier, Place Eugène Bataillon, 34095 Montpellier, France.*
† *Corresponding authors: E-mail address: cynthia.eid@ul.edu.lb (C. Eid) Tel: +961 1 681553; fax: +961 1 686983.*
E-mail address: Mikhael.bechelany@univ-montp2.fr (M. Bechelany). Tel: +33 467149167; fax: +33467149119.

Experiments

1. Synthesis of Graphene oxide

GO was synthesized using an improved Hummers method as reported by Marcano *et al*. [28]. 3g of Graphite powder (Sigma-Aldrich, # 282863, <20μm powder) and 18 g of potassium permanganate (Alfa Aesar, # 30743) has been added slowly in a mixture of 40 mL of phosphoric acid (Sigma-Aldrich, # 30417) and 360 mL of sulfuric acid (ACS reagent, 95.0-98.0%). The solution was then heated to 50° C and stirred for 18 hours. After cooling to room temperature, the solution was poured onto ice (400 mL) with 3 mL of H_2O_2 (30 weight percentage in H_2O, ACS reagent). The solution was then filtered. The filtrate was centrifuged (6000 rpm for 5 min) and the supernatant was decanted away. The mixture was then purified using the protocol of sifting, filtering, centrifugation, decanting with multiple washes followed the procedure described elsewhere [28]. The final solution was vacuum filtered and the solid was placed in an oven for 12 hours to obtain the Graphene oxide (GO).

2. Synthesis of CoFe$_2$O$_4$/GO nanofibers

For the synthesis of CoFe$_2$O$_4$/GO nanofibers, we must first ensure that the Graphene oxide is well dispersed in 2.5 mL of distilled water by sonication for at least 4 hours. Different GO weight amounts (20 mg, 40 mg and 60 mg) have been dispersed in the same water volume. Next, a polymer solution was prepared by dissolving 1.37 g of the solid powder PVP (polyvinylpyrrolidone, MW ≈ 1,300,000, Aldrich) in 14.7 mL of absolute ethanol (EtOH). Then, 1g of iron (III) nitrate nonahydrate ($Fe(NO_3)_3.9H_2O$, MW: 404.00, assay: ≥ 98%, Aldrich) and 0.3052g of cobalt (II) acetate tetrahydrate ($(CH_3COO)_2.Co.4H_2O$, MW: 291.03, assay: ≥ 98%, Aldrich) were added to the polymer solution. After that, 2.5 mL of the GO solution was added with vigorous magnetic stirring for 1.5 h. Finally, 1 mL of acetic acid (ACS reagent, ≥99.7%) was mixed with the previous solution. When water (surface tension ~74.2 mN/m) is present in the solution, the concentration of acetic acid (surface tension ~28.8 mN/m) strongly influences the surface tension of the solution by lowering it and increasing the charge density. Therefore, the electrospinning behavior is improved and no droplets are observed [29,30]. The final homogeneous solution was used in the electrospinning process. The viscous solution thus obtained was drawn into a hypodermic syringe. The positive terminal of a variable high voltage power supply was connected to the needle tip of the syringe while the other was connected to the metallic collector plate. The positive voltage applied to the tip was 25.5 kV, and the distance between the needle tip and the collector was 15 cm. The flow rate was 1 mL/h. When the spinning was completed, the as-prepared fibers were calcined under air at 600°C for 3 hours with a heating rate of 2 °C/min. Table 1 summarizes the names of the fibers prepared with different GO weight amounts after thermal treatment.

3. Physical and chemical Characterizations

The morphology of the samples was analyzed by Field Emission Scanning Electron Microscopy (FESEM, Hitachi S4800, Japan). EDX measurement was carried out using a Zeiss EVO ED15 microscope coupled with a Oxford X-MaxN EDX detector. Samples have been studied by transmission electron microscope (TEM PHILIPS - CM 20). Raman spectra have been obtained from a 'HORIBA Xplora' Raman microscope operating at wavelength λ = 532 nm. The X-ray diffraction (XRD) patterns of the samples were recorded using X-ray diffraction (PAN alytical Xpert- PRO diffractometer equipped with an accelerator detector using Ni-filtered Cu-radiation) with Cu Kα radiation (l = 0.15406nm) at 40 kV and 20 mA. The crystallite size was obtained from the X-ray diffraction pattern using of the Scherrer's formula.

$$D = \frac{k\lambda}{\beta cos\theta} \qquad \text{(Equation 1)}$$

Where D is the grain size (Å), k is a constant equal to 0.94, β is the full width at half maximum (FWHM) (radian) and λ (Å) is the wavelength of the X-rays.

The N_2 sorption-desorption isotherms were measured with a Micromeritrics ASAP 2010 equipment (outgassing condition 200°C-12h). The magnetic properties were analyzed by Superconducting Quantum Interference Device (SQUID) (Quantum design- MPMS XL).

Table 1: Samples (CoFe$_2$O$_4$) prepared with different weight amounts of GO. Samples denoted A are annealed under air.

Mass of GO (mg)	Samples
0	A1
20	A2
40	A3
60	A4

Results and discussion

In order to study the influence of Graphene Oxide (GO) incorporation on the CoFe$_2$O$_4$ nanofibers properties, four different samples have been elaborated and fully characterized: (i) CoFe$_2$O$_4$ without GO (A1), (ii) CoFe$_2$O$_4$ with 20 mg GO weight amount (A2), (iii) CoFe$_2$O$_4$ with40 mg GO weight amount (A3), and (iv) CoFe$_2$O$_4$ with 60 mg GO weight amount (A4). The Atomic Force Microscopy (AFM) performed on GO before the incorporation in CoFe$_2$O$_4$ nanofibers shows the formation of single layers of Graphene Oxide by exfoliation with the thickness of about 1 ± 0.2 nm with a lateral size of approximately 0.4 × 1.0 μm demonstrated a very efficient exfoliation of GO (Supporting Information: Figure S1).

Table 2. Surface area and porosity of nanofibers with different amounts of GO

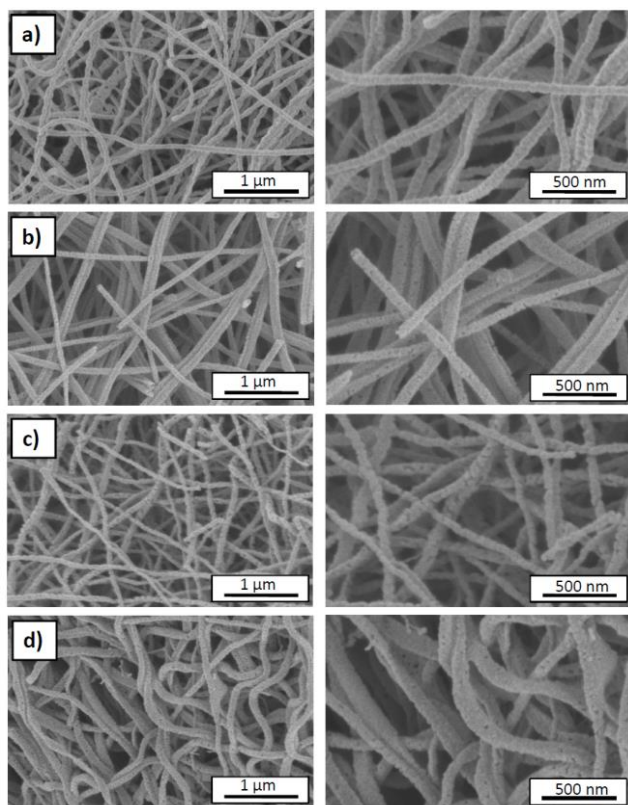| | Samples | | | |
	A1	A2	A3	A4
Surface Area (m²/g)	< 0.01	10.69	12.52	0.90
Pore Volume (cm³/g)	-	0.0225	0.0284	0.0024
Pore Size (Å)	-	84.25	90.86	105.9

Fig 1: SEM images of the $CoFe_2O_4$ / GO annealed nanofibers with various amounts of GO: (a) A1; (b) A2; (c) A3; and (d) A4

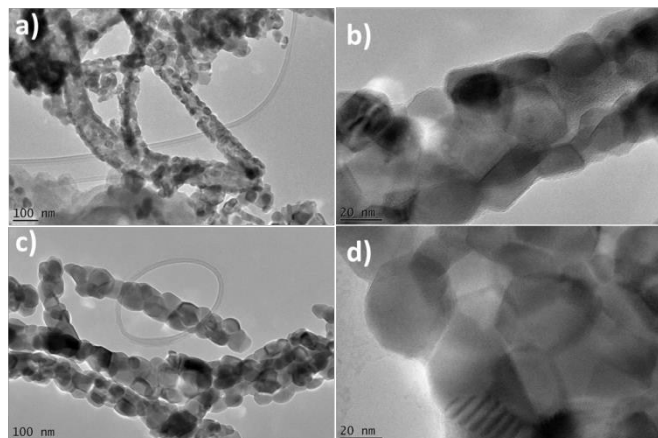**Fig 2.** TEM images of the $CoFe_2O_4$ / GO annealed nanofibers with various amounts of GO: A1 (a, b) and A4 samples (c, d).

The morphology of the annealed nanofibers was examined by scanning electron microscopy (SEM; Figure 1). The one dimensional morphology was maintained after thermal treatment. Moreover, an increase in the pore size is observed with the increase of the amount of GO as confirmed by BET. (Table 2) Annealing the fibers at 600°C could possibly induce the decomposition of some GO monolayers that results in the formation of porosity inside the nanofibers.

High resolution SEM images were used for image analysis. Measured on 100 randomly chosen nanofibers of each sample, the average diameters were measured using the ImageJ, Java-based image processing program. The results are reported as mean ± standard deviation. We calculated an average diameter of (61 ± 21) nm, (108 ± 27) nm, (112 ± 20) nm and (141 ± 23) nm for samples with GO weight amount of 0, 20, 40 and 60 mg respectively. Taking into consideration all the samples prepared with different GO weight amounts, we calculated the variability quantified as the standard deviation/mean (%) [31]. It was found to be 34%, 25%, 18% and 16% for samples A1, A2, A3 and A4 respectively. First, it can be noticed that the average diameter increases with the increase of the amount of GO. This can be an evidence of the successful incorporation of the Graphene oxide in the $CoFe_2O_4$ nanofibers. As for the variability, doping with GO demonstrates a better diameter control of the fibers possibly due to the stability of the jet when the fibers' diameter is higher. Besides, we can easily distinguish the presence of individual particles that confirm the good crystalline structure of the samples.

In order to confirm that GO is really presented inside the nanofibers, SEM-EDX analysis was utilized to determine the chemical compositions of the GO doped-$CoFe_2O_4$ nanofibers. The EDX compositions of the samples are presented in Table 3. It confirms the presence of both cobalt and iron with an atomic ratio of ≈ 1:2. Comparing the GO doped fibers to the pure one, we can notice the increase of the atomic percentage (At (%)) of carbon in the samples A2, A3 and A4. Since the EDX analysis for low atomic number elements such as C and O is not accurately enough, the GO content in the samples could not be estimated with high accuracy.

Table 3. SEM/EDX composition of the different samples: A1, A2, A3 and A4

Samples	Atomic pourcentages			
	Co	Fe	O	C
A1	12.58	27.46	54.87	5.09
A2	13.90	27.29	50.62	8.19
A3	9.73	20.35	59.39	10.53
A4	17.65	33.81	41.12	7.43

Figure 2 illustrates the TEM images of samples A1 and A4. It was found that GO incorporation had a significant effect on the morphology and the crystallinity of $CoFe_2O_4$ nanofibers. They clearly showed that all the nanofibers were composed of nanosized grains and their size changed when GO is incorporated. As is evident from Figures 2b and 2d, the nanograin size increases with the incorporation of GO in the $CoFe_2O_4$ nanofibers. In addition, GO flakes were not detected in the nanofibers using TEM confirming the good dispersion of GO between the nanosized grain. We note here that unlike graphene, GO does not have any define structure.

ARTICLE

because oxidation destroys the initial (002) peak of pristine graphite thus making GO a structureless "amorphous" (carbon based) materials and it could not be detected by selected area diffraction.
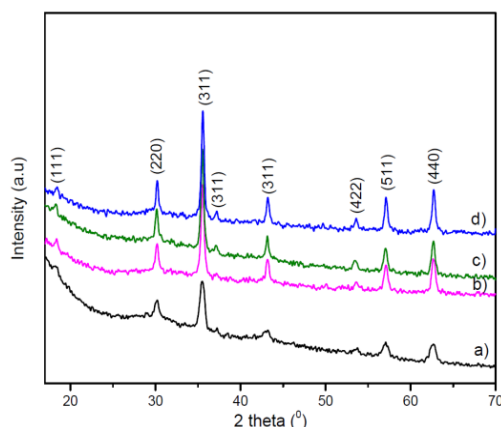

Fig 3. XRD patterns of the samples: (a) A1; (b) A2; (c) A3; and (d) A4
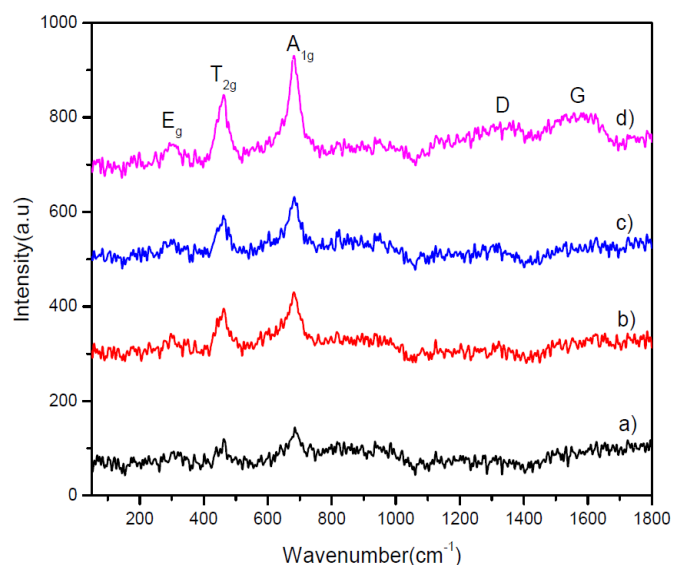

Fig. 4: Raman spectra of the samples: (a) A1; (b) A2; (c) A3; and (d) A4.

The samples' structure was further investigated by XRD. The patterns shown in Figure 3 confirm the presence of the cubic spinel structure for all the samples calcined at $600^{o}C$ and prepared with different amount of GO (JCPDS 03-0864, space group: $Fd3jm$). No impurity phase was found in all the patterns. Seven peaks appear at 2Θ = 18.4°, 30.29°, 35.56°, 43.03°, 53.39°, 57.07° and 62.77° which correspond to (111), (220), (311), (400), (422), (511) and (440) respectively of the crystallized structure of $CoFe_2O_4$.

No peaks were observed indicating the presence of GO. This might be attributed to the highly dispersion and incorporation of GO into the $CoFe_2O_4$ lattice as well as to its amorphous nature [32]. The grain size was determined by the Scherrer's formula [33]. It was found to be 18.95, 28.77, 29.89 and 29.92 nm for the samples A1, A2, A3 and A4 respectively consisting with what has been obtained

by TEM. Compared to the pure $CoFe_2O_4$ nanofibers (Sample A1), doping with GO has enhanced the spinel crystalline structure. Concalves *et al.* suggested that a higher density of oxygen functional groups promoted the dispersion of the gold nanoparticles (NPs) along the Graphene oxide surface and demonstrated the importance of the oxygen groups at the GO surface for the nucleation and growth of Au NPs [34]. In our case, the oxygen functional groups may have promoted the growth of $CoFe_2O_4$ crystallites.

Raman spectroscopy study has been conducted since it is a sensitive tool to detect carbon doped materials. The figure 4 shows Raman spectra of the $CoFe_2O_4$ and $CoFe_2O_4$/GO composite nanofibers calcined at 600°C. Ferrites crystallize in cubic structures belonging to the Fd-3m crystal space group. Active modes for the spinel structure are: A_{1g}, E_g, T_{1g}, $3T_{2g}$, $2A_{2u}$, $2E_u$, $4T_{1u}$ and $2T_{2u}$. Out of these modes, five are Raman active, namely A_{1g}, E_g and $3T_{2g}$. All the Raman spectra of $CoFe_2O_4$ show 3 peaks positioned around $299.65cm^{-1}$, $461.50cm^{-1}$, $681.13cm^{-1}$. These peaks are all characteristic bands of $CoFe_2O_4$ in the frequency range of 0–$1800cm^{-1}$. Assignments of these phonon modes were carried out in accordance with the work performed by Chandramohan *et al.* [35]. Phonon modes at low frequencies ($299cm^{-1}$ and $461cm^{-1}$) are due to the metal ion in the octahedral void (BO_6) and correspond to the symmetric and anti- symmetric bending of oxygen atom in M–O bond (E_g and T_{2g}). Other phonon modes at higher frequency (peak maxima at $681cm^{-1}$), are due to A1g mode involving symmetrical stretching of the oxygen atom with respect to the metal ion in the tetrahedral void. The Raman spectra of the as-prepared GO/$CoFe_2O_4$ nanofibers displays a broad D-band at $1326 cm^{-1}$ and a broad G-band at $1580 cm^{-1}$ for the sample A4, which confirms that the GO was successfully introduced into the nanofibers during electrospinning. The D peak is associated with vibrations of carbon atoms with dangling bonds in plane terminations of disordered graphite and is a breathing mode or k-point photons of A1g symmetry, whereas the G peak corresponds to the first-order scattering of the E2g mode and is related to the vibration of sp2-bonded carbon atoms in a 2D hexagonal lattice [36-38]. These two bands are not visibly distinguished for lower doping although the FTIR results. In addition, the increased intensity of the ferrite bands with the amount of doping is visibly noticed. It confirms how the quantity of GO in the nanofibers affects and promotes the arrangement of the spinel crystalline structure.

The Figure 5 shows the FTIR spectra of pure GO and GO-doped $CoFe_2O_4$ nanofibers. The peaks of GO (Figure 5a) at 3423, 1724, 1612, 1222, 1035 and 968 cm^{-1} are due to the vibration and deformation bands of O-H and C=O stretching vibrations from carbonyl groups, C=C configurable vibrations from the aromatic zooms, C-OH stretching vibrations, C-O vibrations from epoxy groups and C-O vibrations from alkoxy groups, respectively [39]. In the case of $CoFe_2O_4$/GO nanofibers (samples A2, A3 and A4), the bands related to the carbon-containing functional groups (indexed in the Figure) are observed. They start to arise for sample A2 (Figure 5d) and become more pronounced for higher GO amount

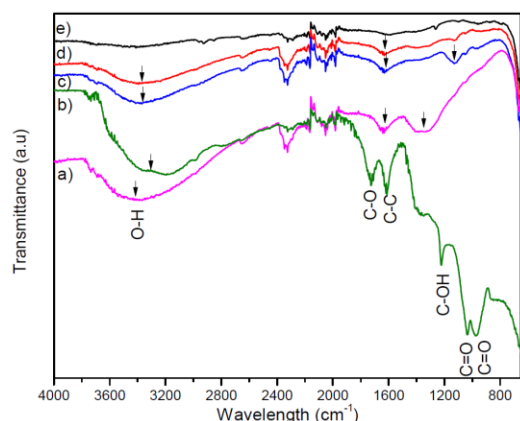indicating the presence of GO in the fibers after the process of air annealing.

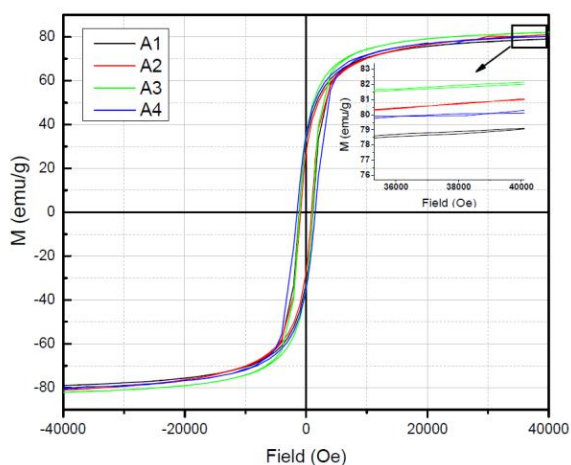**Fig 5:** FTIR spectra of the samples: (a) A1; (b) A2; (c) A3; and (d) A4.

Fig 6: Magnetic hysteresis loops at 300 K of the as-prepared CoFe$_2$O$_{4/}$GO samples: A1; A2; A3; A4.The inset is a magnified view of the curves at high magnetic fields.

The Figure 6 shows the variation of the magnetization for CoFe$_2$O$_4$ nanofibers with different GO doping levels. The curves were obtained at 300 K in a magnetic field range from -40 000 Oe to 40 000 Oe. All samples exhibit hysteresis loops reflecting the ferrimagnetic nature of CoFe$_2$O$_4$. Table 4 summarizes the values of the coercivity, the remnant magnetization and the saturation magnetization for all the prepared samples.

Changes in the coercivity and in the remanence appear random and inconsistent with the doping levels. This can be possibly due to the presence of particle aggregations that could affect the magnetic properties of the materials [4]. Also, many parameters can influence the variation of the coercivity. Besides the crystals' size, the presence of pores plays a significant role [40-41]. It obstructs the coherent rotation of the magnetization and, thus, provokes a reduction in the coercivity as the porosity increases. Since the BET analyses showed an increase in the pore volume for A2 and A3 compared to A4, a reduction in the coercivity was expected.

However, the sample A3 demonstrated better crystallization that could influence itself the increase of the coercivity with respect to A2. As for sample A1, no porosity has been detected (Table 2) which can explain the higher measured coercivity.

On the other hand, the saturation magnetization Ms is higher for the doped nanofibers. It increases with the doping level for samples A1, A2 and A3. For sample A4, Ms becomes lower (≈80 emu/g) than the measured values for samples A2 (≈81 emu/g) and A3 (≈83 emu/g). The saturation magnetization values obtained for the different samples are close to those of bulk cobalt ferrite (≈ 81 emu / g) [40]. Considering the improvement of the crystallinity with the doping level, an enhancement of the saturation magnetization is expected. In fact, since the cubic spinel structure is more complete when doping with GO as noticed in the TEM, XRD and Raman studies, the increased particle size reduces the contribution of the disordered magnetic moments in the boundary surface layer and increases the influence of the well-arranged spins in the particle core under an external magnetic field [4].

Table 4: The remnant magnetization, the coercivity and the saturation magnetization of the CoFe$_2$O$_4$/GO nanofibers calcined under air for 3h at 600°C and prepared with different GO weight amounts.

Sample	Remnant magnetization (emu/g)	Coercivity (Oe)	Saturation magnetization (emu/g) ± Standard error
A1	36	1175	79.24 ± 0.21
A2	31	909	81.05 ± 0.47
A3	38	1102	82.70 ± 0.39
A4	39	1514	80.08 ± 0.71

Conclusions

In conclusion, we have successfully prepared GO-doped CoFe$_2$O$_4$ nanofibers by electrospinning technique while varying the weight amount of GO. The one dimensional morphology was maintained regardless the amount of doping. The SEM images showed an increase in the average diameter with the increase of GO. In fact, the TEM and XRD spectra showed the correlation between the domain size of the crystalline structure of the CoFe$_2$O$_4$ and the GO incorporation effect. A boost of the grain size from 18.95 to 29.92 nm had been recorded when the weight of GO was increased to 60 mg. This result is a direct proof how the higher density of oxygen functional groups in the GO promotes the nucleation and the growth of the ferrite's structure. Also, with increasing the amount of GO, the saturation magnetization of CoFe$_2$O$_4$ was enhanced owing to the increase of the CoFe$_2$O$_4$crystallites' size. These results prove that the GO can play a significant role in the enhancement of the crystalline structure and

ARTICLE   Journal Name

the magnetic properties of the ferrites. Further investigations on the temperature dependences of the magnetization are underway to study the effect of GO on the magnetic transition of the $CoFe_2O_4$.
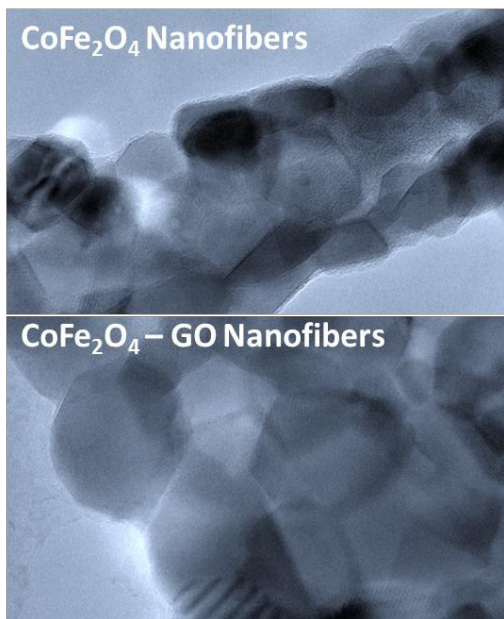
References

1   C. Eid, A. Brioude, V. Salles, J-C Plenet, R. Asmar, Y. Monteil, R. Khoury, A. Khoury and P. Miele, *Nanotechnology*, 2010, **21**, 125701.

2   C. Eid, D. Luneau, V. Salles, R. Asmar, Y. Monteil, A. Khoury and A. Brioude, *J. Phys. Chem. C.,* 2011, **115**, 17643.

3   C. Dong, X. Xiao, G. Chen, H. Guan and Y. Wang, *Mater Lett*, 2014, **123**, 187.

4   Z. Wang, X. Liu, M. Lv, P. Chai, Y. Liu and X. Zhou, *J. Phys. Chem. C* , 2008, **112**, 15171.

5   Y.N Xia and P.D. Yang, *Adv Mater*, 2003, **15**, 351.

6   S. Jiang, G. Duan, E. Zussman, A. Greiner and S. Agarwal, *ACS Appl Mat Interfaces*, 2014, **6**, 5918.

7   R. Dersch, M. Steinhart, U. Boudriot, A. Greiner and J.H. Wendorff, *Polym. Adv. Technol*., 2005, **16**, 276.

8   Z.M. Huang, Y.Z. Zhang, M. Kotaki and S. Ramakrishna, *Compos. Sci. Technol.*, 2003, **63**, 2223.

9   S. Agarwal and S. Jiang, Nanofibers and Electrospinning, Springer Berlin Heidelberg, 2015.

10 M. Sangmanee and S. Maensiri, *Appl Phys A*, 2009, **97**, 167.

11 Z. Wang, X. Liu, M. Lv, P. Chai, Y. Liu, and J. Meng, *J. Phys. Chem. B*, 2008**, 112**, 11292.

12 R. Valenzuela, Magnetic Ceramics, Cambridge University Press, Cambridge, 1994.

13 M. Sugimoto, *J. Am. Ceram. Soc.*, 1999, **82**, 269.

14 R.C. O'Handley, Modern Magnetic Materials—Principles and Applications, Wiley, New York, 2001.

15 Y. Dan, Y. Lu, N.J. Kybert, Z. Luo and A.C. Johnson, *Nano Lett.*, 2009, **9**, 1472.

16 K.I. Bolotin, K. Sikes, Z. Jiang, M. Klima, G. Fudenberg, J. Hone, P. Kim and H. Stormer, *Solid State Commun.*, 2008, **146**, 351.

17 A.A. Balandin, S. Ghosh, W. Bao, I. Calizo, D. Teweldebrhan, F. Miao and C.N. Lau, *Nano Lett.*, 2008, **8**, 902.

18 M.J. McAllister, J.L. Li, D.H. Adamson, H.C. Schniepp, A.A. Abdala, J. Liu, M.Herrera-Alonso, D.L. Milius, R. Car and R.K. Prud'homme, *Chem. Mater.*, 2007, **19**, 4396.

19 S. Stankovich, R.D. Piner, X. Chen, N. Wu, S.T. Nguyen and R.S. Ruoff, *J.Mater.Chem.*, 2006, **16**, 155.

20 S. Stankovich, D.A. Dikin, R.D. Piner, K.A. Kohlhaas, A. Kleinhammes, Y. Jia, Y. Wu, S.B. T.N guyen and R.S. Ruoff, *Carbon, 2007,* **45**, 1558.

21 Y. Yuan, G. Zhang, Y. Li, G. Zhang, F. Zhang and X. Fan, *Polym. Chem.*, 2013, **4**, 2164.

22 O.C. Compton and S.T. Nguyen, *Small*, 2010, **6**, 711.

23 Y. Zhang, B. Chen, L. Zhang, J. Huang, F. Chen, Z. Yang, J. Yao and Z. Zhang, *Nanoscale*, 2011, **3**, 1446.

24 P. Lian, X. Zhu, H. Xiang, Z. Li, W. Yang and H. Wang, *Electrochim.*Acta, 2010, **56,** 834.

25 B. Li, H. Cao, J. Shao, M. Qu and J.H. Warner, *J. Mater. Chem.*, 2011, **21**, 5069.

26 Y.Yao, S. Miao, S. Liu, L.P. Ma, H. Sun and S. Wang, *Chem. Eng. J.*, 2012, **182**, 326.

27 N. Li, M. Zheng, X. Chang, G. Ji, H. Lu, L. Xue, L. Pan and J. Cao, *J. Solid State Chem.*, 2011, **184**, 953.

28 D. C. Marcano, D. V. Kosynkin, Jacob M. Berlin , A. Sinitskii, Z. Sun, A. Slesarev, L. B. Alemany, W. Lu and J. M. Tour, *ACS Nano.*, 2010, **4**, 4806.

29 X. Geng, O-H. Kwon and J. Jang, *Biomaterials*, 2005, **26**, 5427.

30 J-H Song, H-E Kim and H-W Kim, *J Mater Sci: Mater Med.,* 2008, **19**, 95.

29 K. Lin, K-N Chua, G T Christopherson, S. Lim and H-Q Mao, *polymer.*, 2007, **48**, 6384.

30 M. Motlak, N. Barakat, M. ShaheerAkhta, A.M.Hamza, A. Yousef, H.Fouad and O-BongYang, *Ceramics International*, 2015, **41**, 1205.

31 A.L. Patterson, *Physical Review*, 1939, **56**, 978.

32 G. Goncalves, P. Marques, C. M. Granadeiro, H. Nogueira, M. K. Singh and J. Gracio, *Chem. Mater.*, 2009, **21**, 4796.

33 P. Chandramohan , M.P. Snirivasan, S. Velmurugan and S.V. Narasimhan, *J.Solid State* Chem, 2011, **184**, 89.

34 B. Wang, Z. Chen, J. Zhang, J. Cao, S. Wang, Q. Tian, M. Gao and Q. Xu, *Colloids and Surfaces A: Physicochem. Eng. Aspects*, 2014, **457**, 318.

35 M. Fu, Q. Jiao and Y. Zhao, *Materials C characterization*, 2013, **86**, 303.

36 J. Shen, Y. Hu, M. Shi, N. Li, H. Ma and M. Ye, *J. Phys. Chem. C.*, 2010, **114**, 1503.

37 A.V. Murugan, T. Muraliganth and A. Manthiram, *Chem. Mater.*, 2009, **21**, 5004.

38 M.P. Morales, C. de Julián, J.M. González and C.J. Serna, *Journal of Materials Research,* 1994, **9**, 135.

39 P. Tataj, M. P. Morales, S. Veintemillas-Verdaguer, T. Gonzalez-Carreno and C.J Serna, *Handbook of Magnetic Materials, 2006,* **16**, 454.

40 M. Grigorova, H.J. Blytheb, V. Blaskov, V. Rusanov, V. Petkov, V. Masheva, D. Nihtianova, Li.M. Martinez, J.S. Muñoz and M. Mikhov, *Journal of magnetism and magnetic materials,* 1998, **183**, 163.

Table of Content

We report on the synthesis of Cobalt ferrite ($CoFe_2O_4$) nanofibers doped with Graphene oxide (GO) via the electrospinning technique and the study of their chemical, structural and magnetic properties.

RSC Advances

ARTICLE

CoFe₂O₄ Nanofibers

CoFe₂O₄ – GO Nanofibers